

The effects of slope topography on acceleration amplification and interaction between slope topography and seismic input motion



Zezhong Zhang*, Jean-Alain Fleurisson, Frederic Pellet

MINES ParisTech – PSL University, Centre de Géosciences, 35 Rue Saint-Honoré, 77300 Fontainebleau, France

ARTICLE INFO

Keywords:

Slope
Topographic amplification
Wave diffraction

ABSTRACT

Topographic effects are responsible for a multitude of earthquake-related disasters and have been used to explain some extreme recorded acceleration values. In particular, slope topography can aggravate the collapse of buildings in the vicinity of the slope. To evaluate this topographic amplification, numerical simulations were conducted with a homogeneous linear elastic slope model that was vertically subjected to scattering SV seismic waves. The numerical analyses were extended using a Gabor wavelet with different frequencies and numbers of cycles to assess the influence of seismic input motion. The results reveal how the topography affects the acceleration recorded on the ground surface of the slope, both in terms of the amplification factor and the location where the maximum amplification is observed. The maximum acceleration amplification is obtained for the slope angle $\alpha = 32.3^\circ$. Due to variations in the slope angle, the maximum amplification is not necessarily obtained at the slope crest; the slope height substantially affects the amplification magnitude but it does not affect the distribution of the peak amplification when it is larger than the wavelength of the input motion. The wave field at the slope surface could be modified depending on the ratio between the slope height and the wavelength, which affects the distribution of the peak amplification near the slope crest. In general, the results identify the effect of the interaction between slope topography and seismic waves on acceleration amplification.

1. Introduction

During earthquakes, local site conditions, including topography (slopes, ridges, and canyons) and geology (sedimentary, basins, and faults), have significant effects on ground motion characteristics and seismic intensity [1–3]. Site effects can increase or sometimes decrease ground motion acceleration [4], and thus the presence of a sharp relief can significantly aggravate the disastrous consequences of strong seismic motions [5,6]. Many field investigations have been conducted after earthquakes and have taken seismic damage related to local site conditions into consideration, such as the 1989 $M_w = 6.9$ Loma Prieta earthquake, the 1999 $M_w = 7.7$ Chi-Chi earthquake, the 2008 $M_w = 7.9$ Wenchuan earthquake, the 2009 $M_w = 6.3$ L'Aquila earthquake in Italy and the 2010 $M_w = 7.0$ Haiti earthquake [7–11]; these earthquakes triggered numerous landslides associated with site effects due to topographic or geological conditions.

The effects of topography have been used by many researchers to explain the large accelerations observed by field accelerographs. For example, during the 1994 Northridge, California, earthquake, a very high horizontal acceleration peak of 1.58 g was recorded by an analog accelerograph installed at a ridge near the Pacoima Dam, while the

peak accelerations recorded by accelerographs in the surrounding areas were under 0.5 g [12]. A similar observation was made during the destructive Haiti earthquake [13]. Field observations have qualitatively noted that topographic irregularities led to the modifications of seismic ground motion. However, there is a lack of detailed field recording of ground motion along slopes; therefore, it is difficult to truly quantify the effects of topography on ground motion. Numerical modeling analysis has been widely developed to predict ground motion modifications [2,14–16]. The quantitative prediction of acceleration amplification is difficult because of the complexity of the physical phenomena of wave diffraction associated with a combination of topographic and geological effects. There are also differences between field observations or measurements and numerical predictions. Recorded ground motions are often larger than numerical predictions [2,6]. Such discrepancies have been attributed to many factors [17–21] such as the presence of a loose soil layer at the surface, wave-field incident angle and orientation, wave type, and three-dimensional (3D) topography geometry. Another cause of complexity is the location of the monitoring points. Ground motion modification is frequency-dependent and can vary from amplification to de-amplification along the surface of the slope [22]; maximum amplification is not necessarily

* Corresponding author.

E-mail address: zhangzezhong32@gmail.com (Z. Zhang).

located at the exact crest of the slope but could be at a short distance behind the crest [16,23]. Buildings are often located at a distance behind the crest, and thus any acceleration amplification in this region can increase seismic destruction. It is, therefore, necessary to evaluate how the topography affects the acceleration amplification on the ground surface.

Many studies have investigated the influence of topography on acceleration amplification using numerical methods incorporating a slope model with sharp corners [16,24]. However, natural slopes often have smooth edges resulting from weathering and water erosion. Rayleigh waves, inducing ground motion amplification, are generated due to wave diffraction around slope corners [25,26], and it is therefore imperative that we get a better understanding of the effect of slope corner curvature on seismic motion modification, since this could be one of the reasons for the differences between observational data and numerical results.

This paper will focus on characterizing acceleration modification along a slope under seismic loading and evaluating the effects of topography, signal frequency and slope edge curvature on acceleration amplification. First, results from numerical simulations will be presented in order to show typical characteristics of acceleration on the ground surface. Then, effects of the slope angle, slope height and curvature of the slope edge will be assessed through a comparison of the acceleration amplifications for different model configurations. Finally, a comparison of the amplification modifications on the ground surface for different frequencies and different numbers of cycles will be provided to demonstrate the influence of the seismic input motion. For this step, the analyses are based on slopes with different geometrical configurations in terms of slope angle and slope height to investigate the interaction between slope and seismic waves.

2. Numerical models

To characterize amplifications of the acceleration on the ground surface along the slope and behind the crest, a series of numerical simulations were performed using the Finite Difference code FLAC8.0 developed by Itasca [27]. Calculation of the distribution of the acceleration along the slope surface was achieved using a linear elastic soil model a density of $\rho = 2000 \text{ kg/m}^3$, Young's modulus of $E = 500 \text{ MPa}$, Poisson's ratio of $\nu = 0.3$, and Shear wave velocity $V_s = 310 \text{ m/s}$. The typical slope model geometry used in the numerical analysis is shown in Fig. 1.

The seismic input motion is a Gabor wavelet (Fig. 2) with a peak ground acceleration (PGA) of 0.5 m/s^{-2} , which is applied at the base of the slope model as a vertical SV wave. To study the effect of the frequency of the input signal on the acceleration amplification, the wavelet frequency was varied in the range 1–10 Hz. Acceleration time history is given by Eq. (1).

$$a(t) = \sqrt{\alpha e^{-\beta t}} \sin(2f\pi t), \tag{1}$$

where f is the central frequency of the signal, t is time, α , β and γ are parameters controlling the shape of the acceleration time history. Corresponding details are listed in Table 1.

In the numerical model, quiet boundaries and free field boundaries (Fig. 1) are used in order to absorb waves approaching the boundary, thus preventing any wave reflection into the model. The solutions of quiet boundaries were proposed by Lysmer and Kuhlemeyer [28], who set normal and tangential dampers to the base of the model to absorb the incident wave so that it cannot return inside the model. This is an effective way to simulate a half-space boundary. Free field boundaries have the same purpose and employ dampers coupled with grids of the lateral vertical boundaries of the model in order to simulate the conditions of a half-space. The accuracy of the numerical analysis using absorbing boundaries has been verified and is in good agreement with analytical predictions [23].

Rayleigh damping is applied to compute the energy dissipation. The damping equation is given as a matrix [27], which comprises components of the mass (M) and the stiffness (K) matrices:

$$C = \alpha M + \beta K, \tag{2}$$

where α is the proportional constant of the mass matrix and β the proportional constant of the stiffness matrix. The equation will reach minimum damping at the following:

$$\xi_{min} = (\alpha\beta)^{1/2}, \tag{3}$$

and

$$\omega_{min} = (\alpha/\beta)^{1/2}. \tag{4}$$

Although the viscous elements applied in Rayleigh damping are frequency-dependent, the independent frequency response can be considered over a limited frequency range by selecting the appropriate parameters of damping ratio and central frequency. In the current study, a damping ratio of 5% was set for the whole model. The frequency of the seismic input motion is selected as the central frequency.

Usually, the observation points located at the free field boundaries on the left or right side of the model are used as reference points [16,24] to calculate the topographic amplification. However, the accelerations for the two reference points are different because of the difference in the thickness of the material between the reference point and the model base. Therefore, in the present study, the amplification factor was computed as the ratio between the absolute value of the peak horizontal ground motion obtained at a given point of the 2D model and the peak horizontal acceleration observed on the ground surface of a corresponding 1D model. The 1D model was built with the same material and the same depth from the observation point to the base of the corresponding 2D model. Using the same loading and boundary

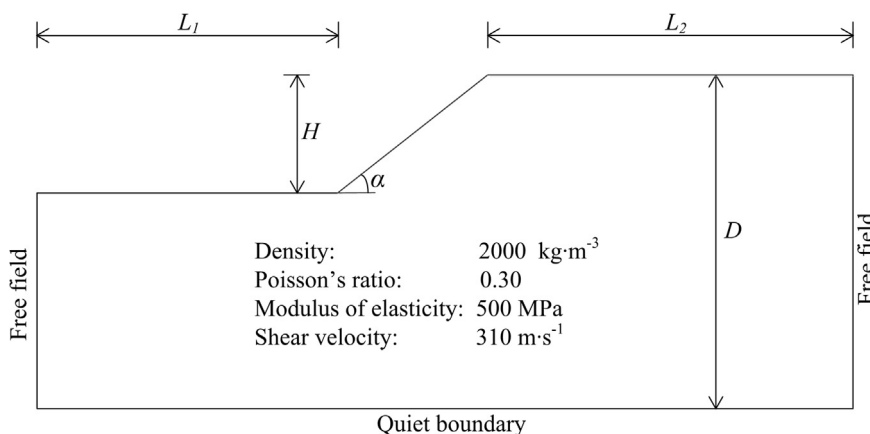


Fig. 1. Geometry of the numerical model for $L_1 = 200 \text{ m}$ and $L_2 = 500 \text{ m}$, $D-H = 150 \text{ m}$.

Download English Version:

<https://daneshyari.com/en/article/6770130>

Download Persian Version:

<https://daneshyari.com/article/6770130>

[Daneshyari.com](https://daneshyari.com)